



**POLITECNICO
MILANO 1863**

SCUOLA DI INGEGNERIA INDUSTRIALE
E DELL'INFORMAZIONE



EXECUTIVE SUMMARY OF THE THESIS

Approach of accelerated SOFC durability test with steam treatment

LAUREA MAGISTRALE IN ENERGETIC ENGINEERING - INGEGNERIA ENERGETICA

Author: MARCO CASTELLI

Advisor: PROF. ANDREA CASALEGNO

Co-advisor: ANKE HAGEN

Academic year: 2021-2022

1. Introduction

Renewable energy sources are gaining popularity as their position in all nations' energy portfolios steadily rises in response to the growing awareness of climate change challenges.

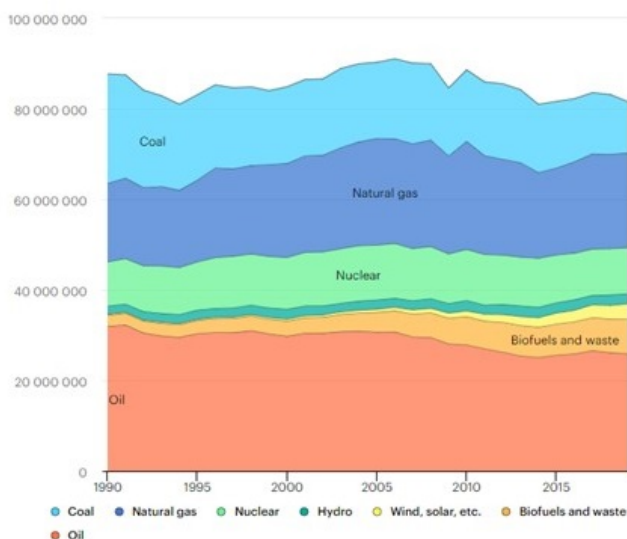


Figure 1: Energy sources in Europe IEA.

Figure 1 illustrates how the situation is in Europe. In fact, oil, natural gas, coal and nuclear energy, are the primary sources, and it is evident that there has been a decline in the use of

coal and oil in recent years. Instead, the world is characterized by three primary sources oil, coal, and natural gas. The Green Deal, which Europe developed in 2020, is a plan for making the EU's economy more sustainable and is based on an integrated energy system. The integrated energy system is based on a cleaner power system with more direct electrification of end-use sectors like industrial heating of buildings and transportation, a cleaner fuel system for difficult-to-electrify sectors like heavy industry, and a "circular" system that is more efficient and where waste energy is gathered and utilized. The Green Deal's goals are then composed of: reaching carbon neutrality by 2050, by 2030 cut the gas emission to 55%, increasing energy efficiency, and integrating renewable energy into the system [1].

At the end of 2018, Europe's ability to produce hydrogen was 11.5 million tons annually. The most popular way to get hydrogen is through on-site captive production, with around two-thirds of all hydrogen production capacity reserved for own consumption. Steam reforming of natural gas is the most often used process to produce hydrogen. According to EU Joint Research Centre, in Europe, electrolysis is utilized when a built-in steam reformer is inadequate or when the capacity is too large for an external supply like a

cylinder or tube trailers. The capacity installed of the electrolyzers is around 1 GW, or 1.6% of the total hydrogen generation capacity. However, the market for electricity to hydrogen is currently small.

The primary sector's demands are divided into 45% in the refinery and 34% in ammonia [1]. These two accounts for 4/5 of the use of hydrogen. The 1% of the use is in the energy sector that is used in combined heat and power (CHP), where hydrogen is burned and produces heat and power, produced on-site, thanks to other processes.

SOC technology presents an opportunity in the electrolyzers and fuel cells world. It is possible to highlight some advantages: thanks to the high operating temperature (600-1000°C), SOC technology obtains high conversion efficiency through the favored thermodynamics and the fast kinetics of the reactions. Then presents the possibility of operating in reverse mode, electrolysis (SOEC), and fuel cell (SOFC) modes. It offers the possibility to use a vast range of fuels, like directly converting hydrocarbons in SOFC mode with higher efficiency than combustion, and CO₂ and H₂O to syngas in SOEC mode. The remaining challenges for technology are costs and lifetime.

The main goal of this research is related to lifetime, specifically to investigate approaches for shortening/accelerating lifetime testing. Steam treatment at OCV was studied as an accelerating factor at the SOFC stack level.

2. SOFC composition

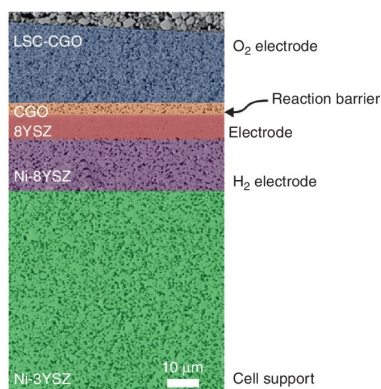


Figure 2: Artificially coloured scanning electron microscope (SEM) image of a DTU-manufactured cross-section solid oxide cell

The stacks' cells are composed by the state of the art of SOFC, called anode-supported cell.

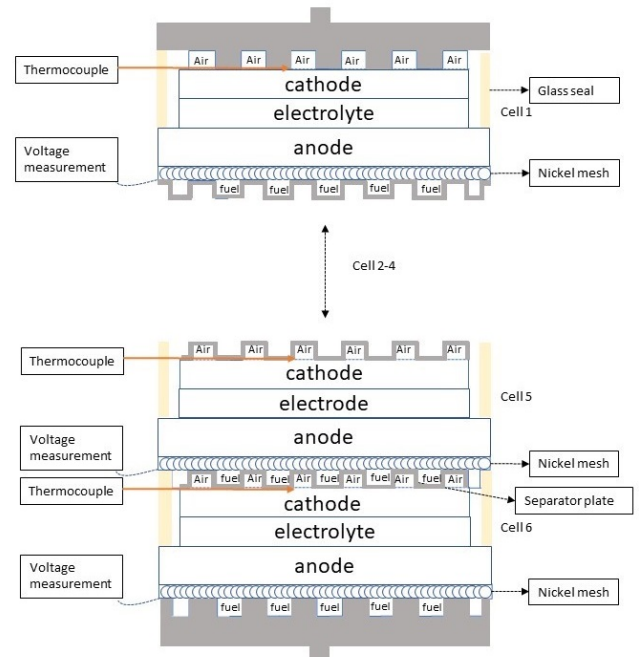


Figure 3: Stack illustration

The air electrode in the cell shown in Figure 2 is made up of *LSC/CGO*, which has a fast oxygen exchange kinetics and a *CGO* barrier to prevent reactions between the air electrode and the electrolyte. The material used to make the electrolyte *8YSZ*, has the ability to transport oxygen ions, while still being gas and electron tight. Additionally, the fuel electrode is made of *Ni-8YSZ*, a bivalent material transporting electrons and oxygen ions from and to the reaction sites.

The stack is made up of 6 cells that are connected by interconnects and stacked on top of one another (SRU), as seen in in figure 3. The SRUs are sealed by glass fiber and a metal housing, stacked under pressure by two end plates. Two cells are linked through a separator plate (interconnect) that serves as the flow field for the airside (cathode) and the fuel source for the anode of the next cell. Additionally, the separator plate transfers electrons from one cell's anode reaction to the cell adjacent to its cathode reaction, distributing them on the surface efficiently.

A thermocouple is positioned differently on the air and fuel in and out, and each cell has its own voltage connection for the measurement (mea-

sured against the ground separator plate). The endplates (grey in figure), which link the stack to the current, have one side that is positive and the other that is negative.

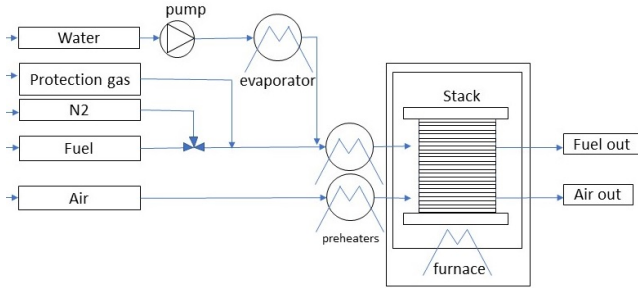


Figure 4: Rig simplification scheme

The stack is then placed within a furnace to maintain a high temperature; for instance, in this test, 750°C. The control scheme for the test station (rig) is shown in figure 4, where the various inner and outlet pipes for fuel and air with preheaters can be seen. Before the test began was installed a pump and a water line to reach a high concentration of steam in fuel in.

3. Methodology

Two tools are used to characterize an electrochemical device: polarization curve, also referred to as I-V curves, and Electrochemical Impedance Spectroscopy (EIS). When operating in a fuel cell or electrolysis mode, polarization curves demonstrate the electric energy that may be produced or absorbed in terms of the potential difference between the two sides of the cell for a given current. From the I-V curve can be extracted e.g. Open Circuit Voltage (OCV), Area Specific Resistance (ASR) of the cell. The OCV, which is the voltage measured at zero current, provides insight into the validity of the data when compared to the predicted value derived from the Nernst equation. Such variations show any unexpected change in operational temperature or supply gas composition. Instead, the ASR is measured in the I-V plot as the slope of the polarization curve at a specific current density or in the impedance plot as the sum of the total resistance and indicates the overall cell resistance incorporating all the various voltage loss effects.

The second tool used is the EIS, which measures the system's impedance to identify the different

phenomenon at different AC frequencies. When interpreting frequency response analysis, it is taken into consideration that the quickest events are ohmic, which occur at extremely high frequencies, followed by kinetic phenomena, which are seen at medium frequencies, and mass transport-related phenomena, which are seen at lowest frequencies. This tool can extract some interesting information from Nyquist and Bode diagrams, where it is possible to underline several impedance contributions related to different processes inside the cell. It was decided not to use any model for simplicity and analyze the ohmic and polarization resistances. As reported before, the ASR can be calculated as the sum of ohmic and polarization resistance, which takes into account the conduction of ions in the electrolyte, conduction of electrons in the electrodes, and contact resistances.

4. Results and discussion

Two stacks were tested, which differ in their prior history and the cell composition on the cathode side; stack A is a new stack using *LSC* in the cathode, whereas stack B presents *LSCF* as cathode, and before this test, the stack was already tested at the DTU laboratory in a co-SOEC mode, with a steady flow of 65% H_2O + 25% CO_2 + 10% H_2 , for 1000-hour period. Then the test, in this study, on Stack A lasted for 500h, and stack B, instead, for 1400 h, both at OCV with 90% H_2O and 10% H_2 , additionally the stacks's measurements were recorded at different concentrations e.g 60/40 H_2/H_2O and 100% H_2 to underline the effect of steam.

5. Stack A (Fresh stack)

Stack A was tested at OCV, with 90% steam and 10% H_2 at 750 °C.

Using the Nyquist plot at 10/90 H_2/H_2O , figure 5, it is possible to see that ohmic resistance has slightly increased, from an average of 0.236 cm^2 to 0.252 cm^2 , with an increase of 6.7%. Instead, a markable rise in polarization resistance can be seen, from an average value of 0.322 cm^2 to 0.43 cm^2 at 502 h. This increase is approximately 33.5%, and in the Bode diagram is present an increase in the high-frequency region. Figure 6 shows the I-V curves and at 0h the OCV point for the various cells is almost identical. Instead the 500 h I-V curves deviate

from the initial polarization curve towards lower voltages, markable at a high current. According to previous publications [4], the rise in ohmic resistance can be attributable to several factors, including Ni migration, which the raise ohmic resistance is caused by the increase in the electrolyte thickness and the O₂-pathway, and/or loss of contact brought on by phase delamination.

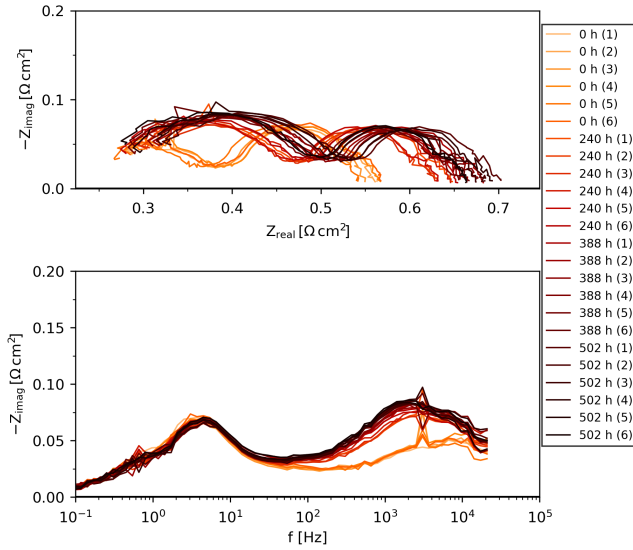


Figure 5: Nyquist and Bode diagram at 10/90 H_2/H_2O T 750°C

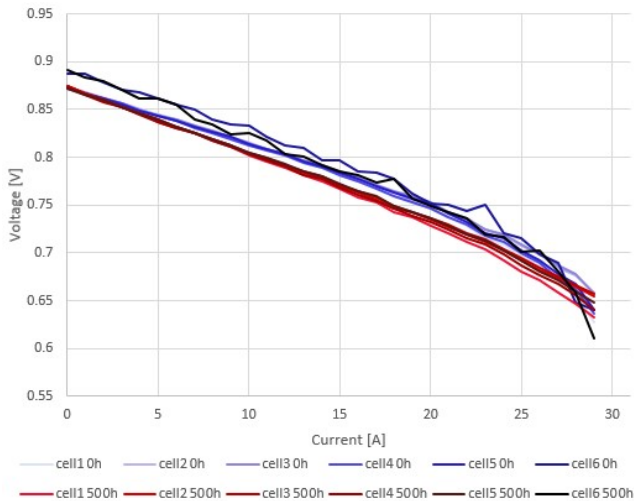


Figure 6: I-V 10/90 H_2/H_2O T 750°C

A deep investigation in previous articles [4] revealed that a decrease in the charge transfer contributions at the fuel electrode is what causes R_p to rise. Significant deviations are seen at high frequencies in the Bode diagram, suggesting a

TPB loss due to Ni migration and/or coarsening. A deep investigation appears to be necessary. However, one theory might be that deterioration occurs both with and without current, as seen in this study as [4] discovered that current speeds up the degradation rate. In the end, all of Mogensen, Trini, and Zekri's ideas were plausible [3, 5, 6]. In fact, it appears that degradation occurs when nickel hydroxide is formed and is either carried to higher pO_2 without current or follows the overpotential when current is introduced. A more thorough investigation must be performed using SEM to support those ideas. The main conclusion of the test is that degradation occurs even without polarization (current density) when applying high steam to the *Ni/YSZ* electrode. Thus, steam is an accelerating parameter for degradation, confirming the findings made at the cell level[4].

6. Stack B (stack with a prehistory of testing)

Stack B was tested at OCV, with 90% steam and 10% H₂ at 750 °C. The results are seen in figure 7 at 60/40 H_2/H_2O : from a starting value of 0.758cm^2 , the average polarization resistance drops by around 13.2%, with a decrease of 6.3% in the first 818 hours and 7.3% in the next 1374 hours.

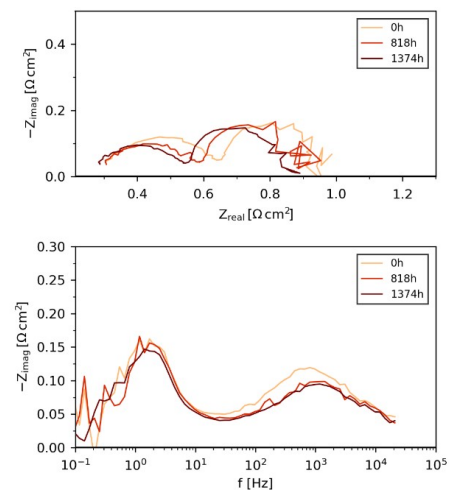


Figure 7: Nyquist and Bode diagram at 60/40 H_2/H_2O T 750°C

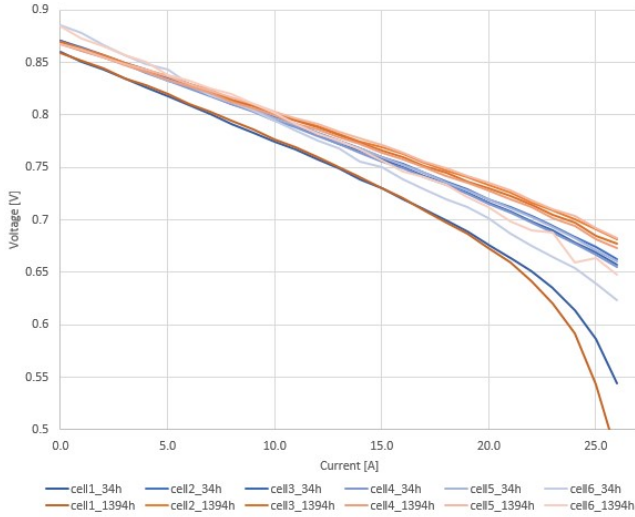


Figure 8: I-V at 10/90 H_2/H_2O T 750°C

Instead, the average ohmic resistance decreases by around 3% overall, increasing by roughly 2% over the course of the first 818 hours from the initial value of 0.2594cm^2 , and then decreasing by about 5.05% to 0.2514cm^2 at 1374 hours. These changes at 900 h could be affected by the laboratory maintenance where the test was forced to go in safety gas, and an air failure happened at 1100h.

As seen in the previous paragraph, the frequency range that is effected is between 100 and 3000 Hz, identified in previous publications as the TPB zone [4]. The Bode plot clearly illustrates these changes with an improvement at 1000 Hz, and it seems that after 818 hours, the impedance reaches a plateau. Figure 8 compares the I-V curve for the different cells before and after the 1394 h with 90% steam. The first thing that can be appreciated is almost no change at OCV, then increasing the current is evident that the I-V curve taken at 1394 h deviate from the curve taken at 34 h, which presents an improvement for all the cells apart from the first cell.

One hypothesis of this behavior was seen in Singhal's article [2] which claims that Ni can catalyze the formation of carbon from hydrocarbons under reducing conditions. Unless sufficient steam and hydrocarbons are used to remove the carbon from the nickel surface. This could explain these test results due to the existence of CO_2 in the stack's prior history of roughly 1000 hours, which CO_2 may coat nickel surfaces, and thanks to a fuel with a high steam content (90%), carbon might be removed from the surface even if

it occurred at two distinct times.

7. Conclusion

In figure 9 are reported polarization and ohmic resistance for both stacks at 60/40 H_2/H_2O . Stack B is depicted by a circle, whereas a triangular dot represents Stack A. The polarization resistance of Stack A degrades during the course of 500 hours, as stated in the previous chapters, whereas the ohmic resistance nearly stays constant with only a small decline.

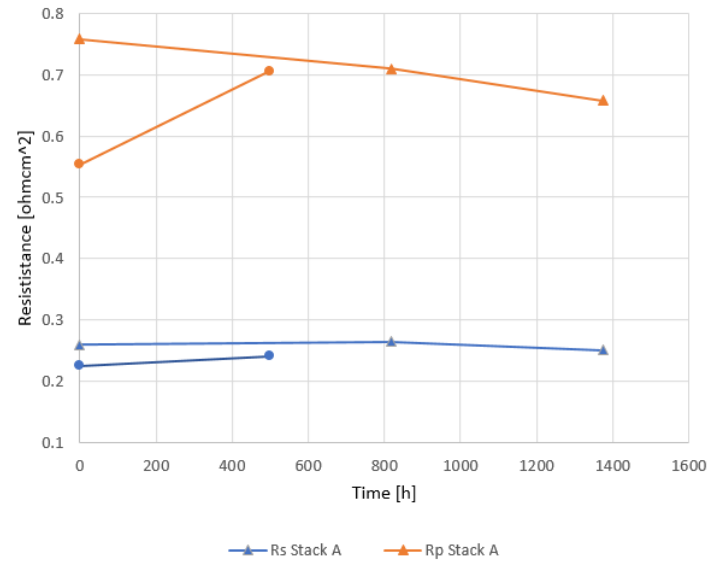


Figure 9: Polarization resistance, ohmic resistance at 60/40 H_2/H_2O at T 750 °C

Instead, for Stack B, there is a decrease in ohmic polarization throughout the 1400 hours, and the ohmic resistance is nearly constant. This figure 9 is interesting for the trend of stack A, which has a huge degradation rate, reaching almost the values of polarization resistance of Stack B at the initial test. According to those patterns, using high steam content causes a significant deterioration as compared to high steam applying it to an older stack, such as Stack B.

From these tests, two main outcomes can be obtained. The first, from stack A, is validated by a previous publication hypothesis[4], where even at OCV under high content of steam it is present a degradation in the ohmic but more in the polarization resistance, that could be caused by a degradation of the triple phase boundary. Second, from stack B, if a stack is tested in co-SOEC before the stem treatment, the steam treatment does not cause degradation and it is possible to

regain some performance lost caused by degradation during the prior operation, for example, carbon deposition.

References

- [1] Clean hydrogen mission-no emission, 2020.
- [2] John T.S. Irvine and Paul Connor. Solid oxide fuels cells: Facts and figures: Past, present and future perspectives for soft technologies. *Green Energy and Technology*, 55, 2013.
- [3] Mogens B. Mogensen, Ming Chen, Henrik Lund Frandsen, Christopher Graves, Anne Hauch, Peter Vang Hendriksen, Torben Jacobsen, Søren Højgaard Jensen, Theis Løye Skafte, and Xiufu Sun. Ni migration in solid oxide cell electrodes: Review and revised hypothesis. *Fuel Cells*, 21:415–429, 10 2021.
- [4] Aiswarya Padinjarethil and Anke Hagen. Identification of degradation parameters in soc using in-situ and ex-situ approaches. *ECS Transactions*, 103:1069–1082, 7 2021.
- [5] M. Trini, A. Hauch, S. De Angelis, X. Tong, P. Vang Hendriksen, and M. Chen. Comparison of microstructural evolution of fuel electrodes in solid oxide fuel cells and electrolysis cells. *Journal of Power Sources*, 450, 2 2020.
- [6] A. Zekri, K. Herbrig, M. Knipper, J. Parisi, and T. Plaggenborg. Nickel depletion and agglomeration in soft anodes during long-term operation. *Fuel Cells*, 17:359–366, 6 2017.